Can transverse mass scaling shed light on the event-activity dependence of Υ-meson production at the LHC?

Iakov Aizenberg,[1] Zvi Citron,[2] and Alexander Milov[1,*]

[1]*Department of Physics and Astrophysics, Weizmann Institute of Science, Rehovot 761001, Israel*
[2]*Department of Physics, Ben Gurion University of the Negev, Beer Sheva 8410501, Israel*

(Received 9 May 2022; revised 11 July 2022; accepted 8 December 2022; published 10 January 2023)

Measurements by the CMS experiment [S. Chatrchyan *et al.* (CMS Collaboration), J. High Energy Phys. 04 (2014) 103; A. M. Sirunyan *et al.* (CMS Collaboration), J. High Energy Phys. 11 (2020) 001] reveal a deficit of charged particle tracks in events with higher $\Upsilon(\mathrm{nS})$ states. This observation is suggested to be a manifestation of the excited bottomonia suppression in pp interactions. Transverse mass (m_{T}) scaling can be implied to check this assumption in an independent way. The scaling has been observed for a wide range of particle species in proton-proton collisions at various energies from the SPS to RHIC and the LHC. The observed scaling is known to be different for baryons and mesons, and this work presents a comprehensive study of the m_{T}-scaling of mesons at LHC energies with a focus on heavier mesons. The study demonstrates patterns in the scaling properties of mesons, which are related to the particle quark content. In particular, light species and ground-state quarkonia obey the same scaling, whereas open-flavor particles deviate from it because their spectra are significantly harder. The magnitude of deviation depends on the flavor of the heaviest quark in the meson. By extending the m_{T}-scaling assumption to the excited bottomonia states, it is observed that the measured cross sections of $\Upsilon(2\mathrm{S})$ and $\Upsilon(3\mathrm{S})$ are reduced by factors of 1.6 and 2.4 compared to the expectation from the scaling. This observation is consistent with recently observed differences between the event-activity dependence of different $\Upsilon(\mathrm{nS})$ meson states.

DOI: 10.1103/PhysRevD.107.014012

I. INTRODUCTION

Based on a statistical thermodynamical approach, it was suggested [1] that hadron production in proton-proton (pp) collisions scales with the transverse mass of the produced particles. Transverse mass is defined as $m_{\mathrm{T}} = \sqrt{p_{\mathrm{T}}^2 + m_0^2}$, where p_{T} is the momentum of the hadron in the plane orthogonal to the collision axis, and m_0 is its rest mass. This scaling was demonstrated experimentally in measurements at the ISR experiment [2]. Although no longer thought to represent a fundamental hadronic temperature as originally proposed, it has since been used by many experiments and phenomenological studies to understand particle production in pp and nucleus-nucleus collisions from the SPS to RHIC and the LHC [3–5]. The original expression of m_{T}-scaling [1] used an exponential form, but it may also be derived based on Tsallis statistics [6] in which a power law provides a better description of particle spectra at higher collision energies ($\sqrt{s}$). Various extensions of the transverse-mass scaling incorporate different assumptions and are capable of describing a broad variety of experimental data with impressive precision [7]. In this article, an assumption of m_{T} scaling is used to provide a qualitative corollary to measurements of Υ mesons made by the CMS experiment in pp collisions [8,9]. CMS observed an intriguing correlation between the order of the $\Upsilon(\mathrm{nS})$-meson state and the multiplicity of charged hadrons measured in pp collisions, and suggested that this may correspond to a suppression of the excited $\Upsilon(\mathrm{nS})$ states. In this analysis, the m_{T}-scaling assumption is used to define a baseline for excited Υ meson production from which suppression could be estimated.

The differential production cross-section can be approximated with the form

$$\frac{\mathrm{d}^2\sigma}{\mathrm{d}y\mathrm{d}m_{\mathrm{T}}} \propto \left(1 + \frac{m_{\mathrm{T}}}{nT}\right)^{-n}, \tag{1}$$

which is derived from Tsallis statistics [7,10]. In addition to m_{T}, the cross-section in the left hand side of Eq. (1) is written as differential also in rapidity, $y = \frac{1}{2}\ln[(E + p_z)/(E - p_z)]$, where E is the energy of a particle and p_z is the momentum component in the direction of colliding protons. In principle, y factorizes from Eq. (1), but in practice a weak dependence of the parameters in the right hand side of Eq. (1) on y

*alexander.milov@weizmann.ac.il

remains in the data [7]. Transverse mass scaling assumes that the exponent n and parameter T are universal for all particles for a given $\sqrt{s}$. It has been shown in many papers that mesons and baryons do not obey the same scaling (e.g., [5] and references therein). The analysis presented in this article considers only mesons. The scaling behavior of heavy mesons is studied in comparison to light quark species, and is used to understand the ratios between excited and ground quarkonia states measured in experiments.

II. EXPERIMENTAL DATA

The experimental data used in this work is drawn from pp collisions at $\sqrt{s} = 7$, 8, and 13 TeV measured by the ALICE [11–23], ATLAS [24–31], CMS [32–42], and LHCb [43–54] experiments. The data are obtained from the HEP database and processed using the following procedure:

(i) Only measurements of mesons are considered.
(ii) Where available, the prompt production component is used. For charmonia states this excludes feed-down contributions from B mesons, but includes the feed-down from decays of heavier charmonium states. These processes may contribute more than 30% of the measured charmonium cross section [33], and the analogous contribution to bottomonium states may be even larger [55].
(iii) For measurements which are corrected using multiple meson polarization assumptions, the results corresponding to the zero polarization assumption are selected.
(iv) Measurements reported within a detector's fiducial acceptance are corrected to the total cross-sections using the zero polarization assumption.
(v) Since particle ratios for quarkonia states considered in this article are typically measured in dilepton decays channels, the particle ratios also include branching ratios.
(vi) Cross-sections measured to rapidity larger than 3 but reported differentially in rapidity are selected with $|y| < 3$ for better consistency with the results measured at midrapidity.

The collected data contains 88 independent measurements of particle species and 18 measurements of the particle ratios, spanning transverse momentum from 0 to 150 GeV and absolute rapidity from 0 to 4.5. Measurements that contain less than 5 data points or spanning less than several GeV in transverse momentum are not used in the analysis. Where multiple measurements of the same particle are reported by the same experiment at the same energy, the measurements typically rely on different statistical samples and therefore are considered to be independent. They are combined using a constant scaling factor applied to one of the measurements. This factor is calculated to account for small differences in the properties of the different measurements, for example the rapidity coverage. The magnitude of the factor is close or equal to unity. Measurements of isospin-partner particles made by the same experiment, and measurements of the same particles performed by different experiments are not combined.

All together, this analysis uses 72 combined data samples of 18 particle species and their isospin partners with 1509 experimental data points, and 15 measurements of particle ratios with 327 data points.

III. FITS

Each data sample is fitted to the functional form given by Eq. (1). Point-by-point uncorrelated uncertainties are used in the fits. Point-by-point fully correlated uncertainties (scaling factors) are not considered because the spectra of different particles are renormalized in the analysis. Other point-by-point correlated uncertainties are shown in the relevant figures but are not input into the fits.

In addition to the general data handling discussed above, several data exclusions are made in the fitting procedure. Measurements of π^0 and $\pi^\pm$ with $p_T < 2$ GeV are excluded based on the considerations discussed in Refs. [5,15]. Low momentum, $p_T < 5$ GeV, Υ meson measurements are also excluded from the fitting because in the low momentum region there is a large contribution from $\chi_b(\mathrm{mP}) \to \Upsilon(\mathrm{nS})\gamma$ decays with $m \geq n$. A correction for feed-down decays from heavier mesons (χ_c, χ_b) is not applied because it cannot be reliably determined from existing data, although it is expected to be similar in magnitude for all $\Upsilon(\mathrm{nS})$ states [56].

Since the fit parameters T and n are strongly correlated with each other, unconstrained fits produce results that are difficult to interpret in a coherent way. Therefore, the parameter T is fixed to 254 MeV for all analyzed particles. This value is obtained from a simultaneous fit to several selected datasets at $\sqrt{s} = 7$ GeV and is close to the value of the same parameter used in [5]. The exponent, n, obtained from the fits is plotted versus the particle rest mass in Fig. 1.

There are several patterns visible in the figure. Particles produced in collisions with higher $\sqrt{s}$ have harder spectra which corresponds to lower values of n, given a fixed T. LHCb results for Υ are higher at each collision energy because they are measured at higher rapidity $2 < |y| < 3$. Comparing results at the same energy shows that n increases with rapidity, reflecting the fact that particle spectra become softer at high rapidity [7]. Several other measurements of light mesons that are made at high rapidity also show higher n, they are not plotted in Fig. 1 for plot clarity.

The magnitude of n obtained from the fits shows a strong dependence on the quark content of the particle. Open heavy flavor mesons $(q||\bar{q})$ demonstrate much harder spectra compared to other species. This holds for all energies and the effect is stronger for open bottom $(b||\bar{b})$ than for open charm $(c||\bar{c})$.

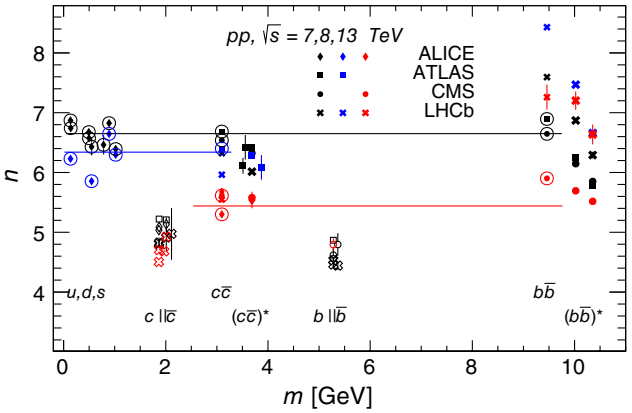

FIG. 1. The mass dependence of the m_T-spectra exponent n for different measured species. Symbol shapes denote experiments, open symbols denote open heavy flavor particles, and larger symbols denote excited quarkonia states. Error bars are uncertainties of the fits. Encircled points indicate the results which are used for common fits of the u, d, s and ground-state $q\bar{q}$ mesons. The results of these fits are shown by horizontal lines. Different colors represent different collision energies.

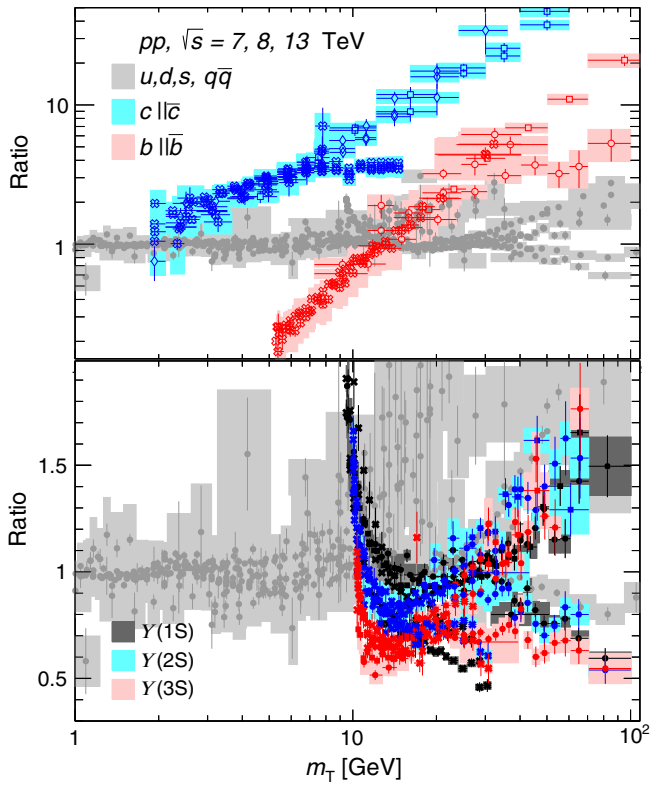

FIG. 2. Measurements used in the common fit are shown in gray. Symbols follow the notation of Fig. 1. Individual curves of $q||\bar{q}$ are scaled with arbitrary factors for visibility.

As has been observed in [7], at LHC and lower energies, light particle species (u, d, s) and quarkonia states follow m_T-scaling, i.e., their spectral distributions can be fitted to Eq. (1), or to the Tsallis form [6], with the same parameters T and n. In a large number of publications the same statement is derived for narrower selections of mesons, e.g., in [4,10,15].

Figure 1 shows that the values of n for u, d, s and ground-state heavy quarkonia ($q\bar{q}$) mesons are similar. However, excited quarkonia states ($(q\bar{q})^\star$) have lower values of n than the ground-state as seen by the ordering $n(\Upsilon(1S)) > n(\Upsilon(2S)) > n(\Upsilon(3S))$. A similar ordering is also observed for charmonia states, $n(J/\Psi) > n(\Psi(2S))$, may be present although the effect is smaller than for bottomonia.

Based on these observations, the values of n for u, d, s and ground-state $q\bar{q}$ mesons measured at midrapidity are fit. The selected datasets are indicated with circles around their markers in Fig. 1. There are 12, 5, and 3 data samples at $\sqrt{s} = 7$, 8, and 13 TeV respectively. The $\sqrt{s} = 7$ TeV values are fit to a linear function which becomes a constant for a chosen value of parameter T. Due to the low number of selected datasets at higher energies, the 8 and 13 TeV data are fit to a constant. The values of $n(\sqrt{s} = 7, 8, 13[\text{TeV}]) = (6.65, 6.34, 5.44)$, and are used in the analysis described below. These values are shown in Fig. 1 by horizontal lines. The quality of the fits and statistical uncertainties associated with the parameters are investigated in detail in a number of similar studies (e.g., [7,57]). In this analysis the robustness of the common fits are checked by changing T by ± 50 MeV, which shifts the points by approximately a unit, but does not change the discussion or conclusions below.

Figure 2 shows the various measurements from all three collision energies, divided by the expectation from m_T-scaling in which n at each collision energy is fixed to the values mentioned above. The points which are used in the common fit are shown in gray, other points are shown in colors. Overall, points shown in gray, demonstrate reasonable agreement with unity, although at high-p_T $q\bar{q}$ spectra tend to rise deviating by up to a factor of 2, somewhat similar to what can be seen in Ref. [7]. Increasing $n(\sqrt{s})$ can partially solve this problem, however, further optimizing the fit would be difficult without knowing the prompt components in the cross sections of heavier species. Taking this into account, and also given the ranges that the measurements cover in particle mass and p_T, the agreement to a common fit shown in the plot can be considered sufficient for the purposes of this analysis.

The upper panel of Fig. 2 compares results measured for $c||\bar{c}$ and $b||\bar{b}$ with the results of the common fit. Individual $q||\bar{q}$ measurements are vertically scaled with arbitrarily chosen factors in the range 0.5–5 for the clarity of the plot. Differences in the slopes are expressions of the observation that $b||\bar{b}$ has harder spectra, compared to $c||\bar{c}$ and other particles, as seen in Fig. 1.

A comparison of the measured $b\bar{b}$ and $(b\bar{b})^\star$ states to the common fit is shown in the lower panel of Fig. 2. This figure shows all data, including measurements at forward rapidity and data points at $p_T < 5$ GeV which are excluded from the fits. The splitting of Υ(nS) points at high-m_T is

due to the $\sqrt{s} = 13$ TeV measurements, whose n is not accurately reflected in the common fit due to a lack of experimental data as seen in Fig. 1. A significant rise for all Υ(nS) states at low p_T, i.e., m_T only slightly above the Υ mass, is clearly visible. The contribution of $\chi_b(1P) \to \Upsilon(1S)$ has been estimated using PYTHIA8 [58] simulations and found to be qualitatively consistent with the large excess at m_T close to the $\Upsilon(1S)$ mass seen in the figure. Higher χ_b states have not been simulated but the similarity of the excess for $\Upsilon(2S)$ and $\Upsilon(3S)$ in the ratio at m_T close to the Υ mass suggests that a significant contribution also of these likely comes from χ_b decays and the nonprompt fraction of the different Υ(nS) states is similar as expected [55,56]. To check the effects of the nonprompt fraction varying between different Υ(nS) states, the PYTHIA8 simulation for the $\chi_b(1P) \to \Upsilon$(nS) processes has been modeled with the same rate as the nonprompt yield of $\Upsilon(1S)$. Then the nonprompt yields into $\Upsilon(1S)$ was increased by additional 20%, i.e., nearly doubled. This is found to not affect the conclusions.

Since the meson ratios at high p_T are constant [29,31,33,38,39,55], $(b\bar{b})^\star$ results shown in the figure are normalized to $b\bar{b}$ at high-p_T by scaling factors. All $\Upsilon(2S)$ results are scaled by 0.9 and all $\Upsilon(3S)$ results by 0.7. The lower panel of Fig. 2 shows that, apart from the rise at low p_T, $\Upsilon(1S)$ follows the trend of particles included in the common fit. On the other hand, compared to $b\bar{b}$ there is a clear deficit of $(b\bar{b})^\star$ states at low and intermediate p_T.

IV. DISCUSSION

The m_T-scaling phenomenon observed at lower $\sqrt{s}$ and at LHC energies for u, d, s mesons approximately holds for heavier $q\bar{q}$ particles in their ground state. Analysis of the LHC data shows that mesons obey or deviate from the scaling depending on the heaviest quark contained in the particle and whether quarks forming the meson are bound in the ground or excited state. Particles with an open charm or bottom have significantly harder spectra than all other particles, and $b||\bar{b}$ mesons have a harder spectra than $c||\bar{c}$ mesons.

Employing m_T-scaling to compare particle spectra distributions is a commonly used technique, as it reproduces well the momentum dependence of a variety of experimentally measured particles [15]. In this article m_T-scaling is used to study the ratios of $(q\bar{q})^\star/q\bar{q}$ as is shown in the upper panel of Fig. 3.

Since the particle ratios are known to only weakly depend on rapidity and $\sqrt{s}$, all available LHC data is shown in the same plot. The p_T dependence of the ratios is not trivial and is challenging for models to reproduce [56]. In this article the data is compared to expectations based on m_T-scaling which are shown with solid lines for the three collision energies. The m_T expectations are normalized to data at $p_T > 50$ GeV, and the uncertainties resulting from the normalization are shown with thin lines. There are clear differences between the expectation and the data for $(b\bar{b})^\star$ species and a significantly better consistency for $(c\bar{c})^\star$.

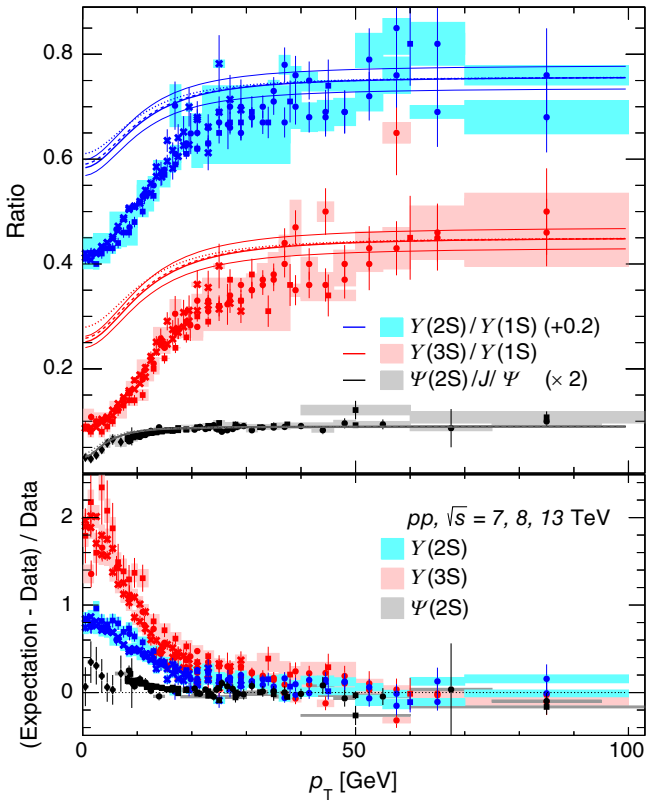

FIG. 3. Upper panel: measured $(q\bar{q})^\star/q\bar{q}$ ratios are shown with markers. $\Psi(2S)$ data is scaled and $\Upsilon(2S)$ data is shifted for plot clarity. Lines are expectations from the m_T-scaling prediction, normalized to the data in the region of $p_T > 50$ GeV. The dashed (dotted) lines correspond $\sqrt{s} = 8\,(13)$ TeV, and finer lines indicate the normalization uncertainty. Lower panel: the difference of the expected value based on m_T-scaling to the measurement divided by the measurement.

To quantify the discrepancies the lower panel shows the particles' "missing fraction" constructed from the ratios. It is the measured value subtracted from the expected value and normalized to the measured, this normalization cancels the ground state production rate and thus the quantity represents the "missing" excited state production equal to $(q\bar{q})^\star_{\text{expected}}/(q\bar{q})^\star_{\text{measured}} - 1$. The normalization uncertainty is added to the systematic uncertainty drawn at each point. The curves show that assuming the m_T-scaling scenario and $\Upsilon(1S)$-meson cross-section, at low p_T the $\Upsilon(2S)$ production expectation is approximately twice as high as the measurement and $\Upsilon(3S)$ is roughly three times higher. Estimation for $\Psi(2S)$ at low p_T is above zero, suggesting that the $(c\bar{c})^\star$ may also be affected, although to a much lesser extent than the Υ case. With the existing data and understanding of the prompt fraction in J/Ψ, a conclusion about $(c\bar{c})^\star$ cannot be drawn with a large degree of certainty. At higher p_T, $\Upsilon(2S)$ and $\Upsilon(3S)$ points are significantly above zero to at least 30 GeV.

The observations reported here may share a common origin with the results reported in [9]. The CMS collaboration measured the production of $\Upsilon(\mathrm{nS})$ mesons at $\sqrt{s} = 7$ GeV as a function of the charged particle multiplicity in the underlying event. CMS observed that events containing $\Upsilon(1\mathrm{S})$ meson measure about two more tracks than events with $\Upsilon(3\mathrm{S})$ and one more track than events with $\Upsilon(2\mathrm{S})$. The CMS collaboration noted, that suppression of the $(b\bar{b})^\star$ states at high multiplicity in pp collisions can produce the measured effect. This assumption is qualitatively consistent with the discrepancy between the $(b\bar{b})^\star$ production rates measured by the LHC experiments and their expectations from the m_{T}-scaling assumption that is plotted in Fig. 3.

If fewer tracks in collisions with $(b\bar{b})^\star$ as observed by CMS, and reduced production of higher $\Upsilon(\mathrm{nS})$ mesons shown in Fig. 3 are two manifestations of the same physics process, it would mean that the measured cross-sections of $\Upsilon(2\mathrm{S})$ and $\Upsilon(3\mathrm{S})$ mesons are 'suppressed' by factors of 1.6 and 2.4 compared to the expectation from the production rates of $\Upsilon(1\mathrm{S})$ scaled by the missing fraction shown in the lower panel of Fig. 3. A 5% uncertainty on these estimates is associated with the normalization uncertainties, and other effects, which are expressed as deviations from the common fit as discussed above, may have a comparable impact on the values. Nevertheless, they are too small to explain the gap between the m_{T}-scaling expected and measured ratios shown in the upper panel of Fig. 3. The mechanism that suppresses the rates of $(b\bar{b})^\star$ may also affect production rates of other $(q\bar{q})^\star$ states, for example, $\Psi(2\mathrm{S})$ shown in Fig. 3, however in this particular case the effect is visibly weaker. Any conclusion about modification of the production rate of the $\Upsilon(1\mathrm{S})$-meson itself, lies outside of the framework of this analysis, because it breaks the m_{T}-scaling assumption. Existing theoretical cross-section calculations [56,59–62] show that the calculations generally better agree with the data for $\Upsilon(1\mathrm{S})$, compared to higher $\Upsilon(\mathrm{nS})$, but these calculations are not available in the low-p_{T} region, where the discrepancy is the largest. Recently the comover interaction model successfully reproduced [63] event multiplicity dependence of the $\Upsilon(\mathrm{nS})$ ratios measured by CMS. Theoretical interpretations of the effect that would simultaneously reproduce the suppression of excited $\Upsilon(\mathrm{nS})$ states and reduction of tracks in the collisions are needed.

V. SUMMARY

A systematic analysis of transverse-momentum distributions of mesons produced in pp collisions at LHC energies suggests that the spectra of light mesons and ground state quarkonia particles have the same spectral shape, given by Eq. (1) with universal parameters T and n for a given collision energy. Open heavy flavor mesons with c-quark in them have significantly harder spectra, and open-flavor b-mesons even harder. Production rates of excited bottomonia states with respect to ground state are significantly suppressed at p_{T} approaching zero, with more suppression measured for the higher excited state. The effect diminishes with increasing p_{T} but remains significant at least up to 30 GeV. Production rates of $\Upsilon(2\mathrm{S})$ and $\Upsilon(3\mathrm{S})$ states are fewer by factors 1.6 and 2.4 respectively, then they would be anticipated from the m_{T}-scaling assumption. This suppression of higher $\Upsilon(\mathrm{nS})$ qualitatively agrees with the effect observed in [8,9] and may be a manifestation of the same physics phenomenon. Production rate of $\Psi(2\mathrm{S})$ is generally consistent with the expectation from J/Ψ, although a smaller-magnitude suppression cannot be excluded. Current theoretical calculations can be advanced by relating the cross-section measurements to the event multiplicity.

ACKNOWLEDGMENTS

Research of Z. C. is supported by the Israel Science Foundation (Grant No. 1946/18). Research of I. A. and A. M. is supported by Israel Academy of Science and Humanity and the MINERVA Stiftung with the funds from the BMBF of the Federal Republic of Germany.

[1] R. Hagedorn, Statistical thermodynamics of strong interactions at high energies, Nuovo Cimento, Suppl. **3**, 147 (1965), http://cds.cern.ch/record/346206.

[2] B. Alper *et al.*, Large angle inclusive production of charged pions at the CERN ISR with transverse momenta less than 1.0 GeV/c, Phys. Lett. **47B**, 75 (1973).

[3] E. L. Bratkovskaya, W. Cassing, and U. Mosel, Meson m_{T}-scaling in heavy ion collisions at SIS energies, Phys. Lett. B **424**, 244 (1998).

[4] B. I. Abelev *et al.* (STAR Collaboration), Strange particle production in pp collisions at $\sqrt{s} = 200$ GeV, Phys. Rev. C **75**, 064901 (2007).

[5] L. Altenkämper, F. Bock, C. Loizides, and N. Schmidt, Applicability of transverse mass scaling in hadronic collisions at energies available at the CERN Large Hadron Collider, Phys. Rev. C **96**, 064907 (2017).

[6] C. Tsallis, Possible Generalization of Boltzmann-Gibbs statistics, J. Stat. Phys. **52**, 479 (1988).

[7] S. Grigoryan, Using the Tsallis distribution for hadron spectra in pp collisions: Pions and quarkonia at $\sqrt{s} = 5$–13000 GeV, Phys. Rev. D **95**, 056021 (2017).

[8] S. Chatrchyan *et al.* (CMS Collaboration), Event activity dependence of $\Upsilon(\mathrm{nS})$ production in $\sqrt{s_{\mathrm{NN}}} = 5.02$ TeV

$p+\mathrm{Pb}$ and $\sqrt{s}=2.76$ TeV pp collisions, J. High Energy Phys. 04 (2014) 103.

[9] A. M. Sirunyan *et al.* (CMS Collaboration), Investigation into the event-activity dependence of $\Upsilon(\mathrm{nS})$ relative production in proton-proton collisions at $\sqrt{s}=7$ TeV, J. High Energy Phys. 11 (2020) 001.

[10] A. Adare *et al.* (PHENIX Collaboration), Measurement of neutral mesons in $\mathrm{p}+\mathrm{p}$ collisions at $\sqrt{s}=200$ GeV and scaling properties of hadron production, Phys. Rev. D **83**, 052004 (2011).

[11] B. Abelev *et al.* (ALICE Collaboration), Neutral pion and η meson production in proton-proton collisions at $\sqrt{s}=0.9$ TeV and $\sqrt{s}=7$ TeV, Phys. Lett. B **717**, 162 (2012).

[12] J. Adam *et al.* (ALICE Collaboration), Multiplicity dependence of charged pion, kaon, and (anti)proton production at large transverse momentum in p-Pb collisions at $\sqrt{s_{\mathrm{NN}}}=5.02$ TeV, Phys. Lett. B **760**, 720 (2016).

[13] J. Adam *et al.* (ALICE Collaboration), Measurement of pion, kaon and proton production in proton-proton collisions at $\sqrt{s}=7$ TeV, Eur. Phys. J. C **75**, 226 (2015).

[14] S. Acharya *et al.* (ALICE Collaboration), Production of ω mesons in pp collisions at $\sqrt{s}=7$ TeV, Eur. Phys. J. C **80**, 1130 (2020).

[15] S. Acharya *et al.* (ALICE Collaboration), Production of light-flavor hadrons in pp collisions at $\sqrt{s}=7$ and $\sqrt{s}=13$ TeV, Eur. Phys. J. C **81**, 256 (2021).

[16] S. Acharya *et al.* (ALICE Collaboration), $\mathrm{K}^{*}(892)^{0}$ and $\phi(1020)$ production at midrapidity in pp collisions at $\sqrt{s}=8$ TeV, Phys. Rev. C **102**, 024912 (2020).

[17] S. Acharya *et al.* (ALICE Collaboration), Measurement of D-meson production at mid-rapidity in pp collisions at $\sqrt{s}=7$ TeV, Eur. Phys. J. C **77**, 550 (2017).

[18] B. B. Abelev *et al.* (ALICE Collaboration), Measurement of quarkonium production at forward rapidity in pp collisions at $\sqrt{s}=7$ TeV, Eur. Phys. J. C **74**, 2974 (2014).

[19] S. Acharya *et al.* (ALICE Collaboration), π^{0} and η meson production in proton-proton collisions at $\sqrt{s}=8$ TeV, Eur. Phys. J. C **78**, 263 (2018).

[20] J. Adam *et al.* (ALICE Collaboration), Inclusive quarkonium production at forward rapidity in pp collisions at $\sqrt{s}=8$ TeV, Eur. Phys. J. C **76**, 184 (2016).

[21] S. Acharya *et al.* (ALICE Collaboration), Inclusive J/Ψ production at midrapidity in pp collisions at $\sqrt{s}=13$ TeV, Eur. Phys. J. C **81**, 1121 (2021).

[22] S. Acharya *et al.* (ALICE Collaboration), Energy dependence of forward-rapidity J/Ψ and $\Psi(2\mathrm{S})$ production in pp collisions at the LHC, Eur. Phys. J. C **77**, 392 (2017).

[23] S. Acharya *et al.* (ALICE Collaboration), Energy dependence of ϕ meson production at forward rapidity in pp collisions at the LHC, Eur. Phys. J. C **81**, 772 (2021).

[24] G. Aad *et al.* (ATLAS Collaboration), Measurement of $D^{*\pm}$, $D^{\pm}$ and $D_{s}^{\pm}$ meson production cross sections in pp collisions at $\sqrt{s}=7$ TeV with the ATLAS detector, Nucl. Phys. **B907**, 717 (2016).

[25] G. Aad *et al.* (ATLAS Collaboration), Measurement of the differential cross-sections of inclusive, prompt and non-prompt J/ψ production in proton-proton collisions at $\sqrt{s}=7$ TeV, Nucl. Phys. **B850**, 387 (2011).

[26] G. Aad *et al.* (ATLAS Collaboration), Measurement of χ_{c1} and χ_{c2} production with $\sqrt{s}=7$ TeV pp collisions at ATLAS, J. High Energy Phys. 07 (2014) 154.

[27] G. Aad *et al.* (ATLAS Collaboration), Measurement of the differential cross-sections of prompt and non-prompt production of J/ψ and $\psi(2\mathrm{S})$ in pp collisions at $\sqrt{s}=7$ and 8 TeV with the ATLAS detector, Eur. Phys. J. C **76**, 283 (2016).

[28] G. Aad *et al.* (ATLAS Collaboration), Measurement of the differential cross-section of B^{+} meson production in pp collisions at $\sqrt{s}=7$ TeV at ATLAS, J. High Energy Phys. 10 (2013) 042.

[29] G. Aad *et al.* (ATLAS Collaboration), Measurement of Υ production in 7 TeV pp collisions at ATLAS, Phys. Rev. D **87**, 052004 (2013).

[30] G. Aad *et al.* (ATLAS Collaboration), K-short and Λ production in pp interactions at $\sqrt{s}=0.9$ and 7 TeV measured with the ATLAS detector at the LHC, Phys. Rev. D **85**, 012001 (2012).

[31] M. Aaboud *et al.* (ATLAS Collaboration), Measurements of $\Psi(2\mathrm{S})$ and $X(3872)\to J/\psi\pi^{+}\pi^{-}$ production in pp collisions at $\sqrt{s}=8$ TeV with the ATLAS detector, J. High Energy Phys. 01 (2017) 117.

[32] V. Khachatryan *et al.* (CMS Collaboration), Prompt and non-prompt J/Ψ production in pp collisions at $\sqrt{s}=7$ TeV, Eur. Phys. J. C **71**, 1575 (2011).

[33] V. Khachatryan *et al.* (CMS Collaboration), Measurement of J/Ψ and $\Psi(2\mathrm{S})$ Prompt Double-Differential Cross Sections in pp Collisions at $\sqrt{s}=7$ TeV, Phys. Rev. Lett. **114**, 191802 (2015).

[34] S. Chatrchyan *et al.* (CMS Collaboration), Measurement of the B^{0} Production Cross Section in pp Collisions at $\sqrt{s}=7$ TeV, Phys. Rev. Lett. **106**, 252001 (2011).

[35] V. Khachatryan *et al.* (CMS Collaboration), Measurement of the B^{+} Production Cross Section in pp Collisions at $\sqrt{s}=7$ TeV, Phys. Rev. Lett. **106**, 112001 (2011).

[36] S. Chatrchyan *et al.* (CMS Collaboration), Measurement of the B_{s}^{0} Production Cross Section with $B_{s}^{0}\to J/\psi\phi$ Decays in pp Collisions at $\sqrt{s}$=7 TeV, Phys. Rev. D **84**, 052008 (2011).

[37] S. Chatrchyan *et al.* (CMS Collaboration), Measurement of the $\Upsilon(1\mathrm{S})$, $\Upsilon(2\mathrm{S})$, and $\Upsilon(3\mathrm{S})$ cross sections in pp collisions at $\sqrt{s}=7$ TeV, Phys. Lett. B **727**, 101 (2013).

[38] V. Khachatryan *et al.* (CMS Collaboration), Measurements of the $\Upsilon(1\mathrm{S})$, $\Upsilon(2\mathrm{S})$, and $\Upsilon(3\mathrm{S})$ differential cross sections in pp collisions at $\sqrt{s}=7$ TeV, Phys. Lett. B **749**, 14 (2015).

[39] S. Chatrchyan *et al.* (CMS Collaboration), J/Ψ and $\Psi(2\mathrm{S})$ production in pp collisions at $\sqrt{s}=7$ TeV, J. High Energy Phys. 02 (2012) 011.

[40] A. M. Sirunyan *et al.* (CMS Collaboration), Measurement of charged pion, kaon, and proton production in proton-proton collisions at $\sqrt{s}=13$ TeV, Phys. Rev. D **96**, 112003 (2017).

[41] A. M. Sirunyan *et al.* (CMS Collaboration), Measurement of quarkonium production cross sections in pp collisions at $\sqrt{s}=13$ TeV, Phys. Lett. B **780**, 251 (2018).

[42] V. Khachatryan *et al.* (CMS Collaboration), Measurement of the differential inclusive B^+ hadron cross sections in pp collisions at $\sqrt{s} = 13$ TeV, Phys. Lett. B **771**, 435 (2017).
[43] R. Aaij *et al.* (LHCb Collaboration), Prompt charm production in pp collisions at $\sqrt{s} = 7$ TeV, Nucl. Phys. **B871**, 1 (2013).
[44] R. Aaij *et al.* (LHCb Collaboration), Measurement of J/Ψ production in pp collisions at $\sqrt{s} = 7$ TeV, Eur. Phys. J. C **71**, 1645 (2011).
[45] R. Aaij *et al.* (LHCb Collaboration), Measurement of $\Psi(2S)$ meson production in pp collisions at $\sqrt{s} = 7$ TeV, Eur. Phys. J. C **72**, 2100 (2012); **80**, 49(E) (2020).
[46] R. Aaij *et al.* (LHCb Collaboration), Measurement of B meson production cross-sections in proton-proton collisions at $\sqrt{s} = 7$ TeV, J. High Energy Phys. 08 (2013) 117.
[47] R. Aaij *et al.* (LHCb Collaboration), Forward production of Υ mesons in pp collisions at $\sqrt{s} = 7$ and 8 TeV, J. High Energy Phys. 11 (2015) 103.
[48] R. Aaij *et al.* (LHCb Collaboration), Measurement of the inclusive ϕ cross-section in pp collisions at $\sqrt{s} = 7$ TeV, Phys. Lett. B **703**, 267 (2011).
[49] R. Aaij *et al.* (LHCb Collaboration), Measurement of $\Psi(2S)$ production cross-sections in proton-proton collisions at $\sqrt{s} = 7$ and 13 TeV, Eur. Phys. J. C **80**, 185 (2020).
[50] R. Aaij *et al.* (LHCb Collaboration), Production of J/Ψ and Υ mesons in pp collisions at $\sqrt{s} = 8$ TeV, J. High Energy Phys. 06 (2013) 064.
[51] R. Aaij *et al.* (LHCb Collaboration), Measurements of prompt charm production cross-sections in pp collisions at $\sqrt{s} = 13$ TeV, J. High Energy Phys. 03 (2016) 159; 09 (2016) 013(E); 05 (2017) 074(E).
[52] R. Aaij *et al.* (LHCb Collaboration), Measurement of the $\eta_c(1S)$ production cross-section in pp collisions at $\sqrt{s} = 13$ TeV, Eur. Phys. J. C **80**, 191 (2020).
[53] R. Aaij *et al.* (LHCb Collaboration), Measurement of forward J/Ψ production cross-sections in pp collisions at $\sqrt{s} = 13$ TeV, J. High Energy Phys. 10 (2015) 172; 05 (2017) 063(E).
[54] R. Aaij *et al.* (LHCb Collaboration), Measurement of Υ production in pp collisions at $\sqrt{s} = 13$ TeV, J. High Energy Phys. 07 (2018) 134; 05 (2019) 076(E).
[55] R. Aaij *et al.* (LHCb Collaboration), Study of χ_b meson production in pp collisions at $\sqrt{s} = 7$ and 8 TeV and observation of the decay $\chi_b(3P) \to \Upsilon(3S)\gamma$, Eur. Phys. J. C **74**, 3092 (2014).
[56] A. Andronic *et al.*, Heavy-flavour and quarkonium production in the LHC era: from proton–proton to heavy-ion collisions, Eur. Phys. J. C **76**, 107 (2016).
[57] G. Bíró, G. G. Barnaföldi, T. S. Biró, and K. Shen, Mass hierarchy and energy scaling of the Tsallis–Pareto parameters in hadron productions at RHIC and LHC energies, EPJ Web Conf. **171**, 14008 (2018).
[58] T. Sjöstrand, S. Ask, J. R. Christiansen, R. Corke, N. Desai, P. Ilten, S. Mrenna, S. Prestel, C. O. Rasmussen, and P. Z. Skands, An introduction to PYTHIA 8.2, Comput. Phys. Commun. **191**, 159 (2015).
[59] H. Han, Y.-Q. Ma, C. Meng, H.-S. Shao, Y.-J. Zhang, and K.-T. Chao, $\Upsilon(nS)$ and $\chi_b(nP)$ production at hadron colliders in nonrelativistic QCD, Phys. Rev. D **94**, 014028 (2016).
[60] N. A. Abdulov and A. V. Lipatov, Bottomonium production and polarization in the NRQCD with k_T-factorization. III: $\Upsilon(1S)$ and $\chi_b(1P)$ mesons, Eur. Phys. J. C **81**, 1085 (2021).
[61] N. A. Abdulov and A. V. Lipatov, Bottomonia production and polarization in the NRQCD with k_T-factorization. II: $\Upsilon(2S)$ and $\chi_b(2P)$ mesons, Eur. Phys. J. C **80**, 486 (2020).
[62] N. A. Abdulov and A. V. Lipatov, Bottomonia production and polarization in the NRQCD with k_T -factorization. I: $\Upsilon(3S)$ and $\chi_b(3P)$ mesons, Eur. Phys. J. C **79**, 830 (2019).
[63] A. Esposito, E. G. Ferreiro, A. Pilloni, A. D. Polosa, and C. A. Salgado, The nature of $X(3872)$ from high-multiplicity pp collisions, Eur. Phys. J. C **81**, 669 (2021).